Stochastic transfer learning strategy for monitoring twin concrete bridges

Leonardo Ferreira[1][0000−0002−4963−8801], Marcus Omori Yano[2][0000−0002−9611−9692], Laura Souza[3][0009−0002−2021−8229], Ionut Moldovan[4,5][0000−0003−3085−0770], Samuel da Silva[2][0000−0001−6430−3746], Rômulo Lopes[3], Carlos Alberto Cimini Jr.[6][0000−0002−6612−0211], and João C.W.A. Costa[3][0000−0003−4482−6886] Elói Figueiredo[4,5][0000−0002−9168−6903]

[1] Universtité Marie et Louis Pasteur, SUPMICROTECH, CNRS, institut FEMTO-ST, F-25000 Besançon, France leonardo.ferreira@femto-st.fr
[2] Universidade Estadual Paulista - UNESP, Faculdade de Engenharia de Ilha Solteira, Departamento de Engenharia Mecânica, Ilha Solteira, Brazil
[3] Universidade Federal do Pará - UFPA, Belém, Brazil
[4] Lusófona University, Faculty of Engineering, Lisbon, Portugal eloi.figueiredo@ulusofona.pt
[5] CERIS - Instituto Superior Técnico, University of Lisbon, Lisboa, Portugal
[6] Universidade Federal de Minas Gerais, Escola de Engenharia, Departamento de Engenharia de Estruturas, Belo Horizonte, Brazil

Abstract. Transfer learning has promised to generalize structural health monitoring (SHM) of bridges, as it permits one to reuse long-term monitoring data across similar structures. Studies have been published using numerical and monitoring data from bridges sharing global similarities. This paper presents the first application of unsupervised transfer learning between twin concrete bridges. The two bridges are located side-by-side, but their construction time is separated by almost three decades. This paper proposes a framework to reuse monitoring data in the undamaged condition from the old bridge to address data scarcity and uncertainty in the training of machine learning algorithms for SHM of the new bridge. To deal with the scarcity of data, a numerical model is developed to simulate the undamaged condition of the new bridge. The model is calibrated using Bayesian inference through Markov-Chain Monte Carlo simulations with the Metropolis-Hastings algorithm. To deal with sources of uncertainty, a transfer learning is used to perform domain adaptation of data sets from both bridges. The results show the numerical model is capable of simulating the dynamics of the new bridge and transfer learning is capable of adapting the distribution domain of the data from the old bridge in such a way that it can be reused to train machine learning algorithms to classify observations from the new bridge.

Keywords: Bridges · Structural Health Monitoring · Unsupervised Transfer Learning · Transfer Learning · Domain Adaptation · Bayesian Inference · Finite Element Modeling · Sensitivity Analysis

1 Introduction

Structural health monitoring (SHM) has long been employed to enhance reliability in bridge management systems, largely because traditional visual inspections often fall short of detecting early-stage damage [1]. These shortfalls have led to a growing interest in automatic damage classification methods, which use monitoring systems to identify the onset of structural problems. Over the past three decades, a statistical pattern recognition paradigm based in machine learning has evolved to handle massive data streams from sensors installed on bridges [2,3]. By focusing on damage-sensitive features, these data-driven methods aim to distinguish between variations due to environmental and operational conditions and those due to genuine structural damage.

When no labeled data about damaged conditions exist, unsupervised learning becomes a critical tool [4]. It assumes that historical data represent mainly the undamaged condition and seeks to identify anomalies that deviate from this norm. Although unsupervised learning can be powerful, the generalization of SHM demands more advanced techniques, leading to the emerging field of transfer learning for SHM. Transfer learning leverages information from a well-characterized source bridge to speed up or improve damage detection in a target bridge with limited data [5].

This paper analyzes two structurally identical bridges, referred to as the "new" and "old" bridges. It is assumed the old bridge has an extensive history of monitoring data, providing a well-understood operational condition, whereas the new bridge has no monitoring data since its commissioning. The new bridge exhibits excessive deformation at its central span, suggesting the presence of damage, making the numerical model essential for reconstructing its undamaged condition. A stochastic finite element (FE) model replicates the pristine state and is updated with limited experimental data in a Bayesian framework. Therefore, using the updated model and domain adaptation within an unsupervised framework, damage detection is achieved even with scarce information on the undamaged state.

Besides Section 1, this paper is organized as follows. Section 2 introduces the feature-based unsupervised transfer learning approach using joint distribution adaptation, the twin concrete bridges over the Itacaiúnas River, and the numerical simulation model. Section 3 details the development and updating of the stochastic numerical model for the new bridge, along with the proposed damage classification framework, comparing training strategies and evaluating domain adaptation performance. Finally, Section 4 presents conclusions and potential future research.

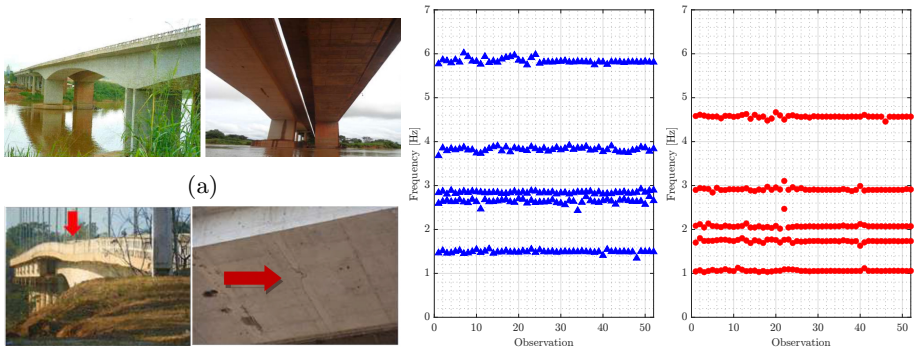

(a) (b) (c) (d)

Fig. 1: Bridges over the Itacaiúnas River: (a) the new (left) and old (right) bridges just after the inauguration of the new one; (b) excessive deflections (left) and potential cracks identified in the new bridge (right); and (c) and (d) one-year experimental natural frequencies of the old (▲) and new (●) bridges, respectively.

2 Methodology

2.1 Twin concrete bridges over the Itacaiúnas River: Structural description and experimental data sets

Two prestressed concrete box girder bridges, located side by side over the Itacaiúnas River in Marabá, Brazil, were built at different times to accommodate increasing local traffic demand (Figure 1). These bridges are considered twins, as they were designed to be structurally identical in dimensions, materials, and appearance. However, exact replication is challenging due to variations in materials, construction methods, and environmental conditions during construction. The old bridge was constructed in the 1980s, while the new one opened to traffic in 2010. Both have a main span of 120 m and two side spans of 70 m each. In 2017, reports of excessive deformation in the new bridge's central span led to a visual inspection. Table 1 presents the first five measured modes for the old bridge and the first six identified modes for the new bridge. Despite their structural similarities, slight differences in natural frequencies are observed.

2.2 Numerical model

As no experimental data are available for the undamaged condition of the new bridge, a numerical model solved using the FE method is developed to estimate it. This model is based on blueprints provided by DNIT and implemented in

Table 1: Comparison between old and new bridges in terms of frequencies. *Note: the letter L is used to specify a lateral mode found in the new bridge only.

Mode	Description	Old bridge [Hz]	New bridge [Hz]
1	First bending	1.47	1.06
1L*	Lateral bending	-	1.42
2	Second bending	2.63	1.74
3	Third bending	2.82	2.08
4	Fourth bending	3.81	2.92
5	Fifth bending	5.83	4.57

CSiBridge v23.3.1. The bridge girder is modeled with beam elements featuring 12 distinct cross-sections. A total of 23 calibration parameters are incorporated, as detailed in Table 2, including spring support stiffness, soil-structure interaction coefficients, and material properties of asphalt and concrete.

Table 2: Numerical model: parameters and search range. *Note: SSI - soil-structure interaction.

Index	Parameter	Unit	Description	Ref. value	Min	Max
1	$k_{i_{U1}}$	MN/m	Longitudinal spring at P1	-	100	1000
2	$k_{i_{U2}}$	MN/m	Lateral spring at P1	-	10	1000
3	$k_{i_{R2}}$	MN/rad	Rotational spring around Y at P1	-	100	1000
4	$k_{i_{R3}}$	MN/rad	Rotational spring around Z at P1	-	100	1000
5	$k_{f_{U1}}$	MN/m	Longitudinal spring at P4	-	10	1000
6	$k_{f_{U2}}$	MN/m	Lateral spring at P4	-	1	1000
7	$k_{f_{R2}}$	MN/rad	Rotational spring around Y at P4	-	10	1000
8	$k_{f_{R3}}$	MN/rad	Rotational spring around Z at P4	-	10	1000
9	$K_{P_{11}}$	MN/m^3	SSI at P1 on soil layer up to 4 m	150	100	200
10	$K_{P_{12}}$	MN/m^3	SSI at P1 on soil layer between 4 and 10 m	200	150	250
11	$K_{P_{13}}$	MN/m^3	SSI at P1 on soil layer between 10 and 16 m	200	150	250
12	$K_{P_{21}}$	MN/m^3	SSI at P2 on soil layer up to 6 m	170	100	250
13	$K_{P_{22}}$	MN/m^3	SSI at P2 on soil layer between 6 and 16 m	200	150	300
14	$K_{P_{31}}$	MN/m^3	SSI at P3 on soil layer up to 11 m	170	100	250
15	$K_{P_{32}}$	MN/m^3	SSI at P3 on soil layer between 11 and 20 m	200	150	300
16	$K_{P_{41}}$	MN/m^3	SSI at P4 on soil layer up to 2 m	10	8	15
17	$K_{P_{42}}$	MN/m^3	SSI at P4 on soil layer between 2 and 4 m	40	30	60
18	$K_{P_{43}}$	MN/m^3	SSI at P4 on soil layer between 4 and 8 m	60	45	75
19	$K_{P_{44}}$	MN/m^3	SSI at P4 on soil layer between 8 and 14 m	200	150	250
20	E_{C25}	GPa	Elastic modulus of concrete C25	29	28	32
21	E_{C35}	GPa	Elastic modulus of concrete C35	33	30	35
22	E_a	GPa	Elastic modulus of asphalt	5.0	4.5	5.5
23	D_a	kg/m^3	Mass density of asphalt	3900	3600	4200

2.3 Feature-based unsupervised transfer learning

This paper considers a feature-based transfer learning approach, as bridge SHM traditionally relies on damage-sensitive features embedding structural knowl-

edge. Transfer learning is implemented through domain adaptation to reduce the distance between source and target features, enabling the classifier to generalize within the latent feature space under a binary classification (undamaged and damaged conditions). JDA, a kernel-based transfer learning method, projects source ($\mathcal{D}_s$) and target ($\mathcal{D}_t$) features into a shared latent space using a nonlinear mapping function $\phi(\cdot)$, minimizing the mismatch between their joint probability distributions. A classifier based on the Mahalanobis squared distance is used in the latent space, and a hypothesis test is established, in which the null hypothesis is the undamaged condition and the alternative hypothesis is the damaged condition [6]. Under this hypothesis, if an observation x_t is extracted from the undamaged condition and it corresponds to a multivariate Gaussian distribution, then the DI will be Chi-squared distributed with d degrees of freedom, $DI \sim \chi^2_d$. Thus, observations from the damaged condition can be defined when their DIs are above a certain level of significance. A level of significance equal to 5% is normally acceptable in the bridge engineering field.

3 Results

3.1 Stochastic model development

An updating process is proposed to develop a stochastic numerical model that replicates the dispersion of experimental natural frequencies. Epistemic uncertainty is addressed by incorporating variance into the model through sampling PDFs for relevant input parameters. Both mode shapes and frequencies serve as target benchmarks for refining the numerical model parameters. Notably, potential damage at the bridge's main span center may influence these frequencies and mode shapes, with bending modes—especially those peaking at the damage location—being most affected. To account for this, the model updating process focuses on mode shapes exhibiting a node at the bridge's center, selecting experimental modes 2 and 4. Additionally, to prevent an overly unconstrained model, the first lateral bending mode (1L) is included as an updating target. Consequently, the process aims to adjust six targets: three mode shapes (1L, 2, and 4) and their corresponding natural frequencies.

The initial step uses Latin hypercube sampling across all 23 parameters to locate regions suitable for optimal solutions. Latin hypercube sampling efficiently covers the entire range of each variable, making it well-suited for high-dimensional spaces with limited samples. Boundaries for these regions are based on literature reference values for material properties (e.g., Souza et al. [7]) or plausible stiffness parameter values, as detailed in Table 2. Mode assurance criteria (MAC) are used to establish numerical-experimental mode correspondence.

A global sensitivity analysis employing Sobol indices [8] is conducted using the UQLab framework for MATLAB [9]. In this analysis, input parameters are perturbed around the optimal candidates identified via Monte Carlo simulations, where parameters are sampled from a uniform distribution centered on the best-fitting values, with bounds extending ±20%. Figure 2 depicts the first-order Sobol indices. The three evaluated modes are predominantly influenced by $k_{i_{U1}}$, $k_{f_{U1}}$, $k_{f_{U2}}$, E_{C25}, and E_{C35}. The results suggests that targeted parameter adjustments could effectively manipulate the bridge's vibrational behavior. Therefore, the next steps are performed using only five parameters: $k_{i_{U1}}$, $k_{f_{U1}}$, $k_{f_{U2}}$, E_{C25}, and E_{C35}.

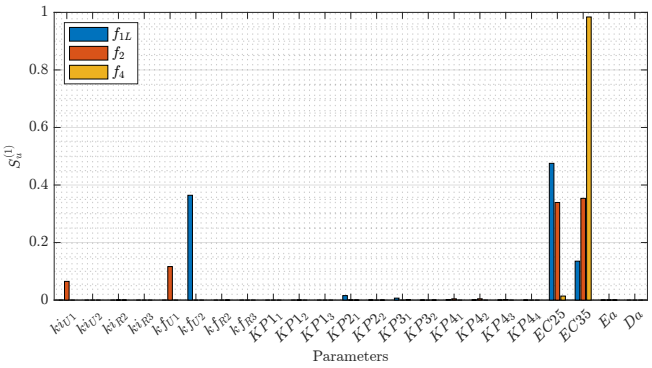

Fig. 2: First order Sobol indices for modes 1L, 2 and 4.

Following the global search and sensitivity analysis, a genetic algorithm (GA) [8] is employed to optimize the relevant parameters identified through the Sobol analysis. Only these selected parameters are refined in the optimization process. Table 3 compares the experimental natural frequencies of the new bridge with those from the numerical model before and after the local search using the genetic algorithm. Notably, the frequency error for the updated modes (1L, 2, and 4) is 0.1%.

The stochastic updating process incorporates epistemic uncertainty into the numerical model, enabling it to replicate the mean experimental response and variability by incorporating PDFs for relevant input parameters. This process follows a Bayesian inference framework using MCMC simulations with the Metropolis-Hastings algorithm[10]. In the genetic algorithm analysis, $k_{i_{U1}}$ and $k_{f_{U1}}$ were identified as correlated variables. Such correlation can destabilize the chain, as the sampling algorithm may counterbalance one variable's variation with the other. To mitigate this issue, only $k_{i_{U1}}$ is retained due to its greater influence over $k_{f_{U1}}$, as indicated by the Sobol indices in Figure 2.

Table 3: Comparison between experimental measurements for the new bridge and numerical model results before and after the genetic algorithm optimization.

Mode	Exp. [Hz]	Initial Num. [Hz]	Initial Error [%]	Initial MAC	Optimized Num. [Hz]	Optimized Error [%]	Optimized MAC
1	1.06	1.18	11.0	1.00	1.16	9.6	1.00
1L	1.42	1.45	2.3	0.68	1.42	0.1	0.67
2	1.74	1.75	0.9	0.79	1.74	0.1	0.79
3	2.08	2.15	3.4	0.97	2.12	1.8	0.96
4	2.92	2.96	1.7	1.00	2.92	0.1	1.00
5	4.57	4.77	4.5	1.00	4.71	3.1	1.00

The prior probability distributions for the variables $\Theta = \{k_{i_{U1}}, k_{f_{U2}}, E_{C25}, E_{C35}\}^T$ are defined as uniform distributions encompassing the average values obtained by the genetic algorithm (GA). Their limits are: $k_{i_{U1}} \sim \mathcal{U}(600, 900)$ [MN/m], $k_{f_{U2}} \sim \mathcal{U}(25, 40)$ [MN/rad], $E_{C25} \sim \mathcal{U}(24, 30)$ [GPa], and $E_{C35} \sim \mathcal{U}(29, 34)$ [GPa]. These ranges include the optimal GA-derived values and provide a search range for the sampling algorithm. Each Markov-Chain Monte Carlo (MCMC) round initializes at the GA-derived mean optimal values $\Theta_i = \{793, 33.8, 27.2, 31.1\}^T$. The variance of the likelihood function is adjusted to maintain a stable acceptance rate between 40% and 50%[10], with the chain simulated over 1000 samples. The first 20% of samples are discarded as burn-in to refine the final PDFs. Figure 3 presents the posterior distributions of the updated parameters.

3.2 Damage classification

The natural frequencies of vibration are used herein as damage-sensitive features. In the original feature space, each observation is composed of the first five natural frequencies of each bridge associated with five bending modes at the bridge deck. For the old bridge, there are 52 experimental observations. For the new bridge, there are 52 experimental measurements corresponding to weekly observations (Figs. 1c and d) and 3000 numerical observations.

Training strategy #1: Experimental data from the source bridge without domain adaptation The classifier is built with a training data set composed of experimental natural frequencies from the source (or old) bridge in its undamaged condition, without any domain adaptation. The test data set comprises 3000 numerical and 52 experimental observations from the target (new) bridge in the undamaged and damaged conditions, respetively. This damage detection strategy intends to assess the usefulness of the data from the old bridge

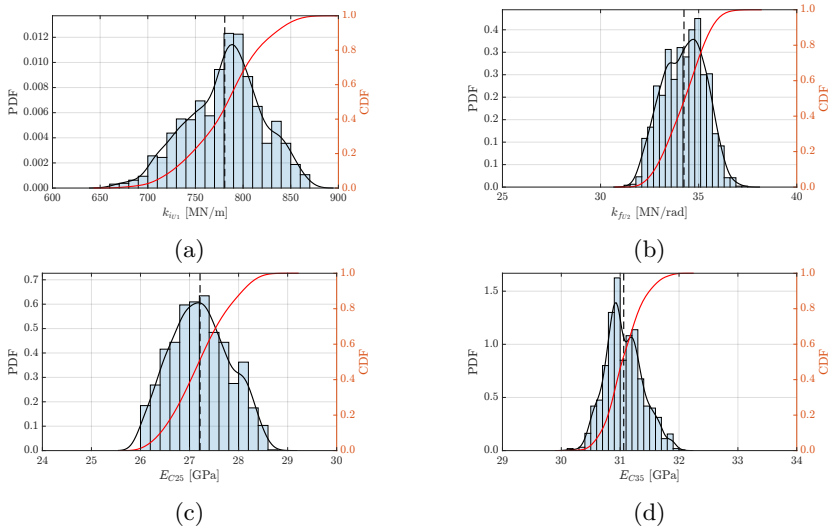

Fig. 3: Sampled posterior probability for the stochastic updating procedure: (a) $k_{i_{U1}}$ distribution; (b) $k_{f_{U2}}$ distribution; (c) E_{C25} distribution; and (d) E_{C35} distribution. In the histograms, the colors represent: Sampled data (▯), kernel density estimate (KDE) (—) and cumulative density function (CDF) (—).

to be directly reused to detect damage in the new bridge. Fig. 4a shows the damage indicator (DI) for each numerical and experimental observation of the new bridge, along with the threshold. The classifier trained without transfer learning is capable of detecting all observations corresponding to the potentially damaged condition (experimental data), at the expense of failing the correct classification of all observations from the undamaged condition derived from the numerical model, yielding an accuracy of 1.64%.

Training strategy #2: Experimental data from the source bridge with domain adaptation The training data set is composed of experimental observations from the source (or old) bridge in the latent feature space. The transformation matrix (using JDA) is built with experimental observations from the source bridge, along with 3000 numerical observations from the target bridge. A total of 3000 numerical observations were used, but it should be noted that no influence on the amount of numerical samples used in the transformation matrix was found. Figure 5 shows the marginal distributions of the source and target in the latent feature space, which highlights an alignment of the mean of the data sets from both bridges in the latent feature space. The test data set comprises all 3000 numerical (undamaged condition) and 52 experimental (damaged condition) observations from the target bridge. Fig. 4b shows the DI for each observation, along with a threshold assuming a level of significance of 5%.

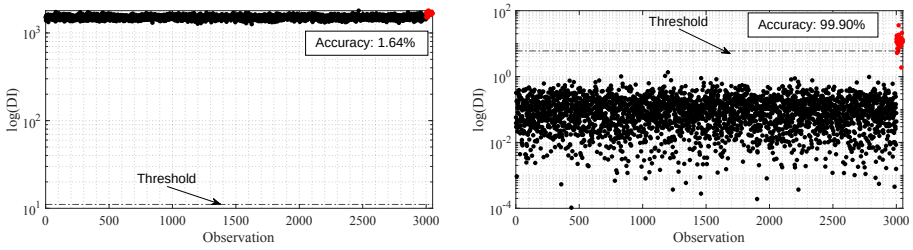

(a) (b)

Fig. 4: Classification performance (damage detection) in the latent feature space for the new bridge data: (a) training strategy #1, and (b) training strategy #2. In these figures, (●) represents "Undamaged - Target" observations, and (●) represents "Damaged - Target" observations.

Almost all observations from the damaged condition are classified as outliers, yielding an accuracy of 99.9%.

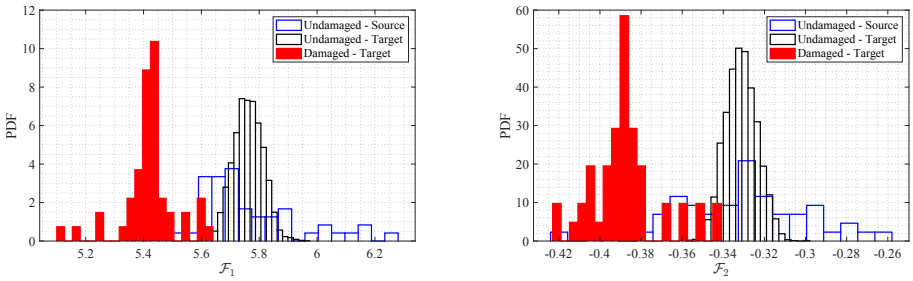

Fig. 5: Marginal distributions of the source and target domains in the latent feature space

4 Conclusions

The proposed framework for unsupervised transfer learning across twin concrete bridges based on data sets from both monitoring and stochastic numerical model with Bayesian calibration provided substantial benefits in addressing data scarcity and different sources of uncertainty (epistemic and random) in the context of bridge SHM. The comparison analysis showed the superiority of a classifier created in the latent feature space backed by transfer learning and domain adaptation, when using both type of data sets (numerical and experimental).

The proposed Bayesian calibration has been able to identify and update relevant input parameters of the numerical model solved by the FE method while accounting for their epistemic uncertainties. The updated mode shapes closely agreed with the experimental ones, including statistical dispersion.

The JDA demonstrated that it had learned the mapping within the shared feature space. The domain adaptation minimized the distance between the two domains (source and target) by approximating the centroids and reducing epistemic uncertainty. The threshold definition based on the source bridge's variance showed to take into account the random uncertainty. The local random variability encoded in the monitoring data from the old bridge was transferred to the classifier of the new bridge, also taking into account the dynamics presented in the numerical data.

References

1. C. Farrar, K. Worden, Structural Health Monitoring: A Machine Learning Perspective, John Wiley & Sons, Ltd, 2013.
2. Z.-W. Chen, S. Zhu, Y.-L. Xu, Q. Li, Q.-L. Cai, Damage detection in long suspension bridges using stress influence lines, Journal of Bridge Engineering 20 (3) (2015) 05014013. doi:10.1061/(ASCE)BE.1943-5592.0000681.
3. E. Figueiredo, J. Brownjohn, Three decades of statistical pattern recognition paradigm for shm of bridges, Structural Health Monitoring 21 (2022) 3018–3054. doi:https://doi.org/10.1177/14759217221075241.
4. M. M. Azad, Y. Cheon, I. Raouf, S. Khalid, H. S. Kim, Intelligent computational methods for damage detection of laminated composite structures for mobility applications: A comprehensive review, Archives of Computational Methods in Engineering (2024). doi:https://doi.org/10.1007/s11831-024-10146-y.
5. M. O. Yano, E. Figueiredo, S. da Silva, A. Cury, Foundations and applicability of transfer learning for structural health monitoring of bridges, Mechanical Systems and Signal Processing 204 (2023) 110766.
6. E. Figueiredo, M. O. Yano, S. da Silva, I. Moldovan, M. A. Bud, Transfer learning to enhance the damage detection performance in bridges when using numerical models, Journal of Bridge Engineering 28 (2023) 04022134. doi:https://doi.org/10.1061/(ASCE)BE.1943-5592.0001979.
7. L. Souza, R. Lopes, E. Figueiredo, I. Moldovan, J. Souza, J. Rabelo, R. Sousa, P. Prazeres, J. Weyl, Ensaios dinâmicos e modelação da ponte sobre o rio itacaiúnas, in: Proc. Encontro Nacional BETÃO ESTRUTURAL - BE2018, 2018.
8. S. Ereiz, I. Duvnjak, J. F. Jimenez-Alonso, Review of finite element model updating methods for structural applications, Structures 41 (2022) 684–723. doi:10.1016/J.ISTRUC.2022.05.041.
9. S. Marelli, B. Sudret, UQLab: A framework for uncertainty quantification in Matlab, in: Vulnerability, Uncertainty, and Risk, ASCE Reston, VA, 2014, pp. 2554–2563. doi:10.1061/9780784413609.257.
   URL https://ascelibrary.org/doi/abs/10.1061/9780784413609.257
10. A. Lye, A. Cicirello, E. Patelli, Sampling methods for solving Bayesian model updating problems: A tutorial, Mechanical Systems and Signal Processing 159 (2021) 107760. doi:https://doi.org/10.1016/j.ymssp.2021.107760.